PHYSICAL REVIEW B VOLUME 44, NUMBER 4 15 JULY 1991-II

Electron-phonon interaction and electron scattering by modified confined LO phonons in semiconductor quantum wells

R. Haupt
Physikalisch-Astronomische Fakultät der Friedrich-Schiller-Universität Jena, Max-Wien-Platz 1, Jena, D/O-6900, Federal Republic of Germany

L. Wendler
Fachbereich Physik der Technischen Universität Merseburg, Geusaer Strasse, Merseburg, D/O-4200, Federal Republic of Germany

(Received 24 September 1990; revised manuscript received 5 February 1991)

An improved model of electron-phonon interaction for longitudinal-optical phonons in layered semiconductor quantum wells is developed. In this simple modified dielectric continuum model, the LO phonons are confined modes having electric and displacement fields that agree with both electrostatics and microscopic models of longitudinal-optical phonons. Numerical results are presented and discussed for the electric fields of these modes. The resulting scattering rates of electrons for emission and absorption of LO phonons in a quantum well are calculated and presented in graphical form.

I. INTRODUCTION

In the past decade, quasi-two-dimensional (Q2D) electron systems in semiconductor heterojunctions and quantum wells (QW's) have attracted much attention. It is well known that the mobility of a quasi-two-dimensional electron gas (Q2DEG) is considerably enhanced at low temperatures by the so-called modulation-doping technique in these structures. This is due to the spatial separation of the Q2DEG from the parent ionized donor impurities, which drastically reduces the ionized impurity scattering. At high temperatures ($T > 40$ K), however, the scattering of electrons by optical phonons plays a dominant role for various electronic properties. Hence, there has been considerable interest in the problem of electron–optical-phonon interaction.

The problem of scattering of electrons by optical phonons in semiconductor microstructures has been treated by a number of authors.[1–9] But in these papers the usual Fröhlich interaction was used,[10] which is based on 3D bulk LO phonons, and only effects of the electron confinement have been properly taken into account. However, the optical phonons are strongly influenced by the presence of the heterointerfaces. The polar or Fröhlich type of electron-phonon interaction (EPI) in polar media is based on the dielectric continuum model.[11] This results from the fact that only long-wavelength optical phonons produce large polarization fields. Using the dielectric continuum model, Fuchs and Kliewer[12] showed that the spectrum of long-wave optical phonons of a polar layer consists of LO and TO phonons, which are confined modes in each individual layer with vanishing influence at the interfaces, and interface phonons with fields mainly localized at the interfaces of the system and decaying exponentially from them. Using the dielectric continuum model, the EPI was considered for various layered structures.[13–28] The general Hamiltonian for this type of EPI in layered and multilayered polar systems including electronic polarizability[21] was applied to different types of single heterostructures,[25] to a double heterostructure,[22] an infinite superlattice,[24] and a semi-infinite superlattice.[23] As in the bulk case, the electrons do not interact with the TO phonons.

Riddoch and Ridley[29] calculated the electron-scattering rates in a thin ionic slab by interaction of the electrons with both types of optical phonons, namely, confined LO and interface phonons. But in this paper the dispersion of the interface phonons was neglected. Wendler *et al.*[30] calculated the electron-scattering rates for semiconductor QW's and superlattices and showed the increasing contribution of the interface phonons if the layer thickness decreases. In the usual dielectric continuum model, the LO phonons are dispersionless and therefore degenerate at the bulk values of the frequency for zero wave vector even in the layered structure. Babiker[31] considered optical modes of a semiconductor QW taking into account the spatial dispersion by an extended dielectric continuum model. In this model he used hydrodynamic boundary conditions at the interfaces, neglecting mixing of LO and TO modes completely.

However, there are indications that the node structure of the confined LO phonons derived from the dielectric continuum model disagree with some experimental Raman-scattering results[32,33] and with results calculated from microscopic models.[34–40] One reason is that the dielectric continuum model is a macroscopic model that corresponds to the long-wavelength limit of optical lattice vibrations. The application of this model to systems with sharp discontinuities at the heterointerface is somewhat problematic. These discrepancies led some authors[41,42] to change the boundary conditions for the fields in the dielectric continuum theory. But this was neither

justified nor in agreement with the electrostatics that is the underlying physics of the dielectric continuum theory.[41,42]

In the present paper we use a modified dielectric continuum model[37] for the LO phonons of layered semiconductor structures, for instance, GaAs-AlAs QW's. The boundary conditions used here agree with both electrostatics and microscopic models. We consider the electron–LO phonon interaction and calculate the electron-scattering rate by interaction with these modified confined LO phonons and compare the results with those for the usual confined LO phonons. We note that the modifications investigated here do not influence the interaction of the electrons with the interface phonons. For the latter case, the theory is developed in Refs. 21, 22, and 24. Further, Raman-scattering experiments show that the dielectric continuum model describes well the interface phonons.[43] Microscopic model calculations for interface phonons also show perfect agreement with the dielectric continuum model results in the low-wave-vector limit.[37]

II. THE DIELECTRIC CONTINUUM MODEL

A. Confined LO phonons

In the local continuum model the LO phonons are described by Maxwell's equations of electrostatics with the lattice dielectric function $\epsilon_\nu(\omega)=\epsilon_{\infty\nu}(\omega_{\mathrm{L}\nu}^2-\omega^2)/(\omega_{\mathrm{T}\nu}^2-\omega^2)$ and with the conventional boundary conditions of electrostatics. $\epsilon_{\infty\nu}$ is the optical (high-frequency) dielectric constant of the layer ν, and $\omega_{\mathrm{L}\nu}$ and $\omega_{\mathrm{T}\nu}$ are the longitudinal- and transverse-optical (LO and TO) -phonon frequency, respectively. If we assume the interfaces of the layered structure to be perpendicular to the z axis, the translational invariance in the x-y plane allows the introduction of two-dimensional Fourier series. We have applied Born–von Kármán periodic boundary conditions in the x-y plane with the unit area A. $\mathbf{x}_\parallel=(x,y,0)$ and $\mathbf{q}_\parallel=(q_x,q_y,0)$ are the two-dimensional position and wave vector in the x-y plane, respectively. The usual boundary conditions for the fields are the continuity of the electric-field components $E_\parallel(\mathbf{q}_\parallel,z)$ and $\epsilon_\nu(\omega)E_z(\mathbf{q}_\parallel,z)$ across the interfaces of the structure and noninfinite $\mathbf{E}(\mathbf{q}_\parallel,z)$ at $z=\pm\infty$.

Maxwell's equations contain different types of polarization eigenmodes of the layered system: p- and s-polarized TO phonons, p-polarized interface phonons, and p-polarized LO phonons.

Here we are only interested in the LO phonons that are p-polarized. The nonzero components of the electric field $\mathbf{E}$ of the p-polarized modes (transversal magnetic waves) are

$$\mathbf{E}(\mathbf{q}_\parallel,z)=(E_\parallel(\mathbf{q}_\parallel,z),0,E_z(\mathbf{q}_\parallel,z)) \tag{1}$$

using a Cartesian-coordinate system with the axis along $\{\mathbf{e}_\parallel,\mathbf{e}_s,\mathbf{e}_z\}$. Here, $\mathbf{e}_\parallel=\mathbf{q}_\parallel/|\mathbf{q}_\parallel|$ is the unit vector in the propagation direction of the optical-phonon mode in the x-y plane and $\mathbf{e}_s$ is orthogonal to $\mathbf{e}_\parallel$ in this plane. According to Fourier transformation, we get from Maxwell's equations inside each layer the wave equation of the p-polarized modes:

$$\epsilon_\nu(\omega)\left[\frac{d^2}{dz^2}-q_\parallel^2\right]E_\parallel(\mathbf{q}_\parallel,z)=0\ . \tag{2}$$

The two components of the electric field are related to each other by

$$E_z(\mathbf{q}_\parallel,z)=-\frac{i}{q_\parallel}\frac{d}{dz}E_\parallel(\mathbf{q}_\parallel,z) \tag{3}$$

with $q_\parallel=|\mathbf{q}_\parallel|$. LO phonons occur at those particular frequencies $\omega=\omega_{\mathrm{L}\nu}$ where $\epsilon_\nu(\omega)=0$. Hence, we have inside the layer $\nabla\times\mathbf{E}=\mathbf{0}$ but not necessarily $\nabla\cdot\mathbf{E}=0$. For a layered system of different polar materials we have different LO phonons: $\omega=\omega_{\mathrm{L}\nu}$ for $\epsilon_\nu(\omega_{\mathrm{L}\nu})=0$ and $\epsilon_{\nu'}(\omega_{\mathrm{L}\nu})\neq 0$ for $\nu\neq\nu'$ having the LO phonon frequencies of each bulk material.

Further, with $\epsilon_\nu(\omega_{\mathrm{L}\nu})=0$, Eq. (2) is satisfied inside the layer ν for arbitrary fields $\mathbf{E}_{\mathrm{L}\nu}$. But outside the layer ν [$\epsilon_{\nu'}(\omega_{\mathrm{L}\nu})\neq 0$], the electric field must satisfy

$$\left[\frac{d^2}{dz^2}-q_\parallel^2\right]E_\parallel(\mathbf{q}_\parallel,z)=0\ . \tag{4}$$

The boundary condition for $\epsilon_\nu E_{z\mathrm{L}\nu}$ requires that the field $E_{z\mathrm{L}\nu}$ outside the layer ν is zero at the interfaces of the layer ν. To satisfy Eq. (4) the field $\mathbf{E}_{\mathrm{L}\nu}$ must vanish identically outside the layer ν, hence the field component $E_{\parallel\mathrm{L}\nu}$ vanishes at the boundaries of the layer ν. Finally, we have

$$E_{\parallel\mathrm{L}\nu}^m(\mathbf{q}_\parallel,z)=-\frac{i}{\epsilon_0}C_{\mathrm{L}\nu}^m\times\begin{cases}\cos(q_\nu^m z), & -a_\nu/2<z<a_\nu/2\\ 0 \quad \text{otherwise}\ ;\end{cases} \tag{5}$$

$$E_{z\mathrm{L}\nu}^m(\mathbf{q}_\parallel,z)=\frac{q_\nu^m}{\epsilon_0 q_\parallel}C_{\mathrm{L}\nu}^m\times\begin{cases}\sin(q_\nu^m z), & -a_\nu/2<z<a_\nu/2\\ 0 \quad \text{otherwise}\ ;\end{cases} \tag{6}$$

with $C_{\mathrm{L}\nu}^m$ a normalization constant,

$$q_\nu^m=\frac{\pi}{a_\nu}m\ ;\quad m=1,2,3,\ldots$$

and a_ν is the thickness of the layer ν.

For the calculation of the electron-phonon interaction in Sec. III, the electric fields of the confined LO phonons must be orthonormalized according to[21]

$$\int_{-\infty}^{\infty}dz\frac{\Theta_\nu(\omega_{\mathrm{L}\nu})}{\omega_{p\nu}^2}\mathbf{E}_{\mathrm{L}\nu}^{m*}(\mathbf{q}_\parallel,z)\mathbf{E}_{\mathrm{L}\nu}^{m'}(\mathbf{q}_\parallel,z)=\delta_{m,m'} \tag{7}$$

with

$$\Theta_\nu(\omega_{\mathrm{L}\nu})=\frac{9\epsilon_{\infty\nu}^2}{(\epsilon_{\infty\nu}+2)^2} \tag{8}$$

and

$$\omega_{p\nu}^2=\frac{9\epsilon_{\infty\nu}}{(\epsilon_{\infty\nu}+2)^2}(\omega_{\mathrm{L}\nu}^2-\omega_{\mathrm{T}\nu}^2)\ . \tag{9}$$

Using the fields of the usual confined LO phonons, Eqs. (5) and (6), and the normalization relation (7), we obtain for the normalization constant

$$C^m_{\mathrm{L}\nu}=\left[\frac{2}{a_\nu}\frac{\omega^2_{\mathrm{L}\nu}-\omega^2_{\mathrm{T}\nu}}{\epsilon_{\infty\nu}}\frac{q^2_\parallel}{q^2_\parallel+(q^m_\nu)^2}\right]^{1/2}. \tag{10}$$

Hence, the LO phonons of a layered system are composed of ordinary dispersionless bulk LO phonons that propagate to the interfaces of the system and are backscattered from them. At the interfaces the influence of these modes vanishes due to the interference of incident and backscattered waves. This is the physical reason for the discreteness of the z component of the wave vector $\mathbf{q}$ of the LO phonons of a layer. Hence, in the usual dielectric continuum model the LO phonons of layered systems are confined modes having standing-wave character inside the layer in which they exist. There is an important difference between the strongly localized LO phonons of layered systems and ordinary 3D bulk phonons. Whereas for the 3D bulk LO phonons the 3D phonon wave vector starts at $|\mathbf{q}|=0$, for the confined LO phonons wave vectors smaller than $|\mathbf{q}|=\pi/a_\nu$ are forbidden, because they are "quantized" with $q^m_\nu=(\pi/a_\nu)m$. The relation between the electric field and the relative ionic displacement field for LO phonons is given by[24]

$$\mathbf{w}(\mathbf{x},\omega_{\mathrm{L}\nu})=\frac{(\epsilon_0\omega^2_{\mathrm{T}\nu}(\epsilon_{s\nu}-\epsilon_{\infty\nu}))^{1/2}}{\omega^2_{\mathrm{T}\nu}-\omega^2_{\mathrm{L}\nu}}\mathbf{E}(\mathbf{x},\omega_{\mathrm{L}\nu}), \tag{11}$$

where $\epsilon_{s\nu}$ is the static (low-frequency) dielectric constant of the layer ν. Hence, the relative ionic displacement is proportional to the electric field of the LO phonon.

B. Modified confined LO phonons

The LO phonons of the standard dielectric continuum model have the following discrepancies from microscopic models. One difference is that the discrete values of the wave vector in the z direction $q^m_\nu=\pi m/a_\nu$ of the dielectric continuum model now become[35,38,39] $q^m_\nu=\pi m/(N+1/2)a_0$, where N is the number of atomic bilayers of Ga and As inside the GaAs layer and Al and As inside the AlAs layer, for instance, and a_0 is the width of the bilayer, i.e., one-half of the lattice constant. That means that the LO phonons of the microscopic model have a very small penetration depth in the neighboring semiconductor layer of roughly one or two atomic monolayers. Hence, this is only a microscopic correction in atomic scale. In the microscopic model there is a maximum value of nodes and, hence, $m_{\max}=N$. But such an upper limit does not exist for the macroscopic model. Here the complete set of LO modes is given by $m=1,2,\ldots,\infty$, which in the microscopic sense is nonphysical. A further difference between the standard dielectric continuum model, described above, and microscopic models results from different boundary conditions. Microscopic models yield the continuity of the relative ionic displacement field $\mathbf{w}$ at the heterointerfaces. Because $\mathbf{w}\sim\mathbf{E}$ [Eq. (11)], these microscopic boundary conditions result in the continuity of both $E_\parallel$ and E_z at the heterointerfaces. In the standard dielectric continuum model, however, the boundary conditions at the interfaces are those from electrodynamics, i.e., the continuity of $E_\parallel$ and $\epsilon_\nu(\omega)E_z$ and not necessarily of E_z. In the case of LO phonons [which means for $\epsilon_\nu(\omega_{\mathrm{L}\nu})=0$, where $E^m_{z\mathrm{L}\nu}$ is equal to zero outside the layer ν], $E^m_{z\mathrm{L}\nu}$ of Eq. (6) is in general nonzero at the interfaces inside the layer ν. This discontinuity of $E^m_{z\mathrm{L}\nu}$ at the interfaces violates the boundary condition for E_z and w_z resulting from microscopic calculations. Hence, the electric fields of the LO phonons resulting from both models differ slightly. We note that for interface modes such a discrepancy does not occur and the results of both the macroscopic and microscopic models agree very well.[37]

In a microscopic model, the long-wave optical phonons have the following physical properties, which are absent in the usual dielectric continuum model: (i) LO phonons have a very small penetration depth in the neighboring semiconductor; (ii) their relative ionic displacement field is continuous across the interfaces; and (iii) there is a mixing of LO and interface modes for a finite, nonzero wave vector because the spatial dispersion is included.

In this paper we want to overcome the most important point, point (ii). To do this we construct a set of orthonormalized eigenfunctions of the LO phonons fulfilling both the boundary conditions of electrodynamics and the boundary condition of the continuity of $\mathbf{w}$. We note that this procedure guarantees that for both types of forces, the short-range interatomic forces and the long-range Coulomb forces, the boundary conditions are satisfied. Hence, we overcome the problems of Refs. 41 and 42, namely, that their boundary conditions contradict the electrodynamics, and the problem that the fields of the modified LO phonons are not orthogonal.[37,44]

From microscopic calculations a possible system of eigenfunctions for symmetric modes ($m=1,3,5,\ldots$) is given by[37]

$$E^m_{\parallel\mathrm{L}\nu}(\mathbf{q}_\parallel,z)=-\frac{i}{\epsilon_0}C^m_{\mathrm{L}\nu}\times\begin{cases}1+(-1)^{(m-1)/2}\cos(q^m_\nu z), & -a_\nu/2<z<a_\nu/2\\ 0 \quad \text{otherwise}\end{cases} \tag{12}$$

and

$$E^m_{z\mathrm{L}\nu}(\mathbf{q}_\parallel,z)=(-1)^{(m-1)/2}\frac{q^m_\nu}{\epsilon_0 q_\parallel}C^m_{\mathrm{L}\nu}\times\begin{cases}\sin(q^m_\nu z), & -a_\nu/2<z<a_\nu/2\\ 0 \quad \text{otherwise}\end{cases} \tag{13}$$

with the changed wave-vector component $q^m_\nu=(\pi/a_\nu)(m+1)$ so that additionally the boundary condition

$E^m_{zL\nu}(\mathbf{q}_\parallel,z)|_{z=\pm a_\nu/2}=0$ is satisfied. For the antisymmetric modes ($m=2,4,6,\ldots$) the following ansatz is possible:

$$E^m_{\parallel L\nu}(\mathbf{q}_\parallel,z)=-\frac{i}{\epsilon_0}(-1)^{m/2}C^m_{L\nu}\times\begin{cases}\sin(q^m_\nu z)-b^m_\nu z, & -a_\nu/2<z<a_\nu/2\\ 0 \quad \text{otherwise}\end{cases} \tag{14}$$

and

$$E^m_{zL\nu}(\mathbf{q}_\parallel,z)=-(-1)^{m/2}\frac{q^m_\nu}{\epsilon_0 q_\parallel}C^m_{L\nu}\times\begin{cases}\cos(q^m_\nu z)-b^m_\nu/q^m_\nu, & -a_\nu/2<z<a_\nu/2\\ 0 \quad \text{otherwise}\end{cases}, \tag{15}$$

where the constants q^m_ν and b^m_ν are determined by the boundary conditions that both $E_\parallel$ and E_z vanish at the heterointerfaces at $z=\pm a_\nu/2$:

$$\tan\left[\frac{a_\nu}{2}q^m_\nu\right]=\frac{a_\nu}{2}q^m_\nu \tag{16}$$

and

$$b^m_\nu=\frac{q^m_\nu}{\left[1+\left[\frac{a_\nu}{2}q^m_\nu\right]^2\right]^{1/2}}\ . \tag{17}$$

Equation (16) gives a series of solutions for q^m_ν, where $q^m_\nu<(\pi/a_\nu)(m+1)$ is valid. For $m\to\infty$ we have $q^m_\nu\to(\pi/a_\nu)(m+1)$. The eigenfunctions (12)–(15) of the modified model have the property that the lowest possible value π/a_ν for the wave-vector component q_z in the usual model is forbidden for the modified model. Hence, in comparison with the standard model for the wave-vector component $q_z=q^m_\nu$ of the modified model for symmetric modes, an amount of exactly π/a_ν is added, and for antisymmetric modes, an amount of slightly smaller than π/a_ν is added.

If one wants to derive the Hamiltonian of the LO phonons and the Hamiltonian of the EPI, it is necessary to have a system of orthonormal eigenfunctions. Unfortunately, the systems (12)–(15) are not orthogonal [according to Eq. (7)]. In particular, the different symmetric modes are not orthogonal to each other. This is also true for the antisymmetric modes. But, of course, the symmetric modes are orthogonal to the antisymmetric modes. It is possible to orthogonalize this system of functions with the help of Schmidt's orthogonalization method. We can treat this procedure for the symmetric and antisymmetric modes independently. For the three lowest symmetric LO phonon modes, the orthonormalized eigenfunctions for $-a_\nu/2<z<a_\nu/2$ are given by the following.

For $m=1$,

$$E^1_{\parallel L\nu}(\mathbf{q}_\parallel,z)=-\frac{i}{\epsilon_0}C^1_{L\nu}[1+\cos(q^1_\nu z)]\ , \tag{18}$$

$$E^1_{zL\nu}(\mathbf{q}_\parallel,z)=\frac{q^1_\nu}{\epsilon_0 q_\parallel}C^1_{L\nu}\sin(q^1_\nu z)\ ; \tag{19}$$

for $m=3$,

$$E^3_{\parallel L\nu}(\mathbf{q}_\parallel,z)=-\frac{i}{\epsilon_0}C^3_{L\nu}[b_{30}+b_{32}\cos(q^1_\nu z)-\cos(q^3_\nu z)]\ , \tag{20}$$

$$E^3_{zL\nu}(\mathbf{q}_\parallel,z)=\frac{1}{\epsilon_0 q_\parallel}C^3_{L\nu}[b_{32}q^1_\nu\sin(q^1_\nu z)-q^3_\nu\sin(q^3_\nu z)]\ ; \tag{21}$$

for $m=5$,

$$E^5_{\parallel L\nu}(\mathbf{q}_\parallel,z)=-\frac{i}{\epsilon_0}C^5_{L\nu}[b_{50}+b_{52}\cos(q^1_\nu z)+b_{54}\cos(q^3_\nu z)+\cos(q^5_\nu z)]\ , \tag{22}$$

$$E^5_{zL\nu}(\mathbf{q}_\parallel,z)=\frac{1}{\epsilon_0 q_\parallel}C^5_{L\nu}[b_{52}q^1_\nu\sin(q^1_\nu z)+b_{54}q^3_\nu\sin(q^3_\nu z)+q^5_\nu\sin(q^5_\nu z)]\ , \tag{23}$$

with

$$b_{30}=\frac{z_1}{z_2},\quad b_{32}=-\frac{z_5}{z_3}\ ,$$
$$b_{50}=\frac{z_1z_2}{z_3z_4-z_5^2},\quad b_{52}=-\frac{z_2z_5}{z_3z_4-z_5^2},\quad b_{54}=\frac{z_1z_5}{z_3z_4-z_5^2} \tag{24}$$

and

$$z_1=a^2_\nu q^2_\parallel+4\pi^2,\quad z_2=a^2_\nu q^2_\parallel+16\pi^2\ ,$$
$$z_3=3a^2_\nu q^2_\parallel+4\pi^2,\quad z_4=3a^2_\nu q^2_\parallel+16\pi^2\ , \tag{25}$$
$$z_5=2a^2_\nu q^2_\parallel,\quad z_6=a^2_\nu q^2_\parallel+36\pi^2\ .$$

According to the normalization condition (7), the normalization constants $C^m_{L\nu}$ are determined to be

$$C^1_{L\nu}=C^0_{L\nu}\left[\frac{z_5}{a_\nu z_3}\right]^{1/2}, \tag{26}$$

$$C^3_{L\nu}=C^0_{L\nu}\left[\frac{z_5z_3}{a_\nu(z_3z_4-z_5^2)}\right]^{1/2}, \tag{27}$$

$$C^5_{L\nu}=C^0_{L\nu}\left[a_\nu\left[b^2_{50}+\frac{z_1}{z_5}b^2_{52}+\frac{z_2}{z_5}b^2_{54}+\frac{z_6}{z_5}\right]\right]^{-1/2}, \tag{28}$$

with

$$C^0_{\mathrm{L}\nu}=\left[\frac{\omega^2_{\mathrm{L}\nu}-\omega^2_{\mathrm{T}\nu}}{\epsilon_0^2\epsilon_{\infty\nu}}\right]^{1/2} . \tag{29}$$

In the case of the antisymmetric LO phonons, the three lowest orthonormalized eigenfunctions in the region $-a_\nu/2<z<a_\nu/2$ are as follows.

For $m=2$,

$$E^2_{\parallel\mathrm{L}\nu}(\mathbf{q}_\parallel,z)=\frac{i}{\epsilon_0}C^2_{\mathrm{L}\nu}[b_{2,-1}z+\sin(q^2_\nu z)] , \tag{30}$$

$$E^2_{z\mathrm{L}\nu}(\mathbf{q}_\parallel,z)=\frac{1}{\epsilon_0 q_\parallel}C^2_{\mathrm{L}\nu}[b_{2,-1}+q^2_\nu\cos(q^2_\nu z)] ; \tag{31}$$

for $m=4$,

$$E^4_{\parallel\mathrm{L}\nu}(\mathbf{q}_\parallel,z)=-\frac{i}{\epsilon_0}C^4_{\mathrm{L}\nu}[b_{4,-1}z+b_{4,1}\sin(q^2_\nu z)+\sin(q^4_\nu z)] , \tag{32}$$

$$E^4_{z\mathrm{L}\nu}(\mathbf{q}_\parallel,z)=-\frac{1}{\epsilon_0 q_\parallel}C^4_{\mathrm{L}\nu}[b_{4,-1}+b_{4,1}q^2_\nu\cos(q^2_\nu z)+q^4_\nu\cos(q^4_\nu z)] ; \tag{33}$$

for $m=6$,

$$E^6_{\parallel\mathrm{L}\nu}(\mathbf{q}_\parallel,z)=\frac{i}{\epsilon_0}C^6_{\mathrm{L}\nu}[b_{6,-1}z+b_{6,1}\sin(q^2_\nu z)+b_{6,3}\sin(q^4_\nu z)+\sin(q^6_\nu z)] , \tag{34}$$

$$E^6_{z\mathrm{L}\nu}(\mathbf{q}_\parallel,z)=\frac{1}{\epsilon_0 q_\parallel}C^6_{\mathrm{L}\nu}[b_{6,-1}+b_{6,1}q^2_\nu\cos(q^2_\nu z)+b_{6,3}q^4_\nu\cos(q^4_\nu z)+q^6_\nu\cos(q^6_\nu z)] , \tag{35}$$

with

$$\begin{aligned} b_{2,-1}&=-b^2_\nu , \\ b_{4,-1}&=b^2_\nu A_{24}-b^4_\nu , \\ b_{4,1}&=-A_{24} , \\ b_{6,-1}&=b^2_\nu(A_{26}-A_{24}A_{46})+b^4_\nu A_{46}-b^6_\nu , \\ b_{6,1}&=A_{24}A_{46}-A_{26} , \\ b_{6,3}&=-A_{46} , \end{aligned} \tag{36}$$

where

$$A_{24}=\frac{C'^2_2}{C'^2_{24}},\quad A_{26}=\frac{C'^2_2}{C'^2_{26}},\quad A_{46}=\frac{(C^4_{\mathrm{L}\nu})^2}{C^2_{46}} , \tag{37a}$$

$$C^2_{46}=\frac{C'^2_{24}C'^2_{26}C'^2_{46}}{C'^2_{24}C'^2_{26}-C'^2_2C'^2_{46}} , \tag{37b}$$

and

$$C'^2_{KN}=(C^0_{\mathrm{L}\nu})^2\frac{12}{a^3_\nu b^K_\nu b^N_\nu} , \tag{38a}$$

$$C'^2_K=(C^0_{\mathrm{L}\nu})^2\left[\frac{a^3_\nu(b^K_\nu)^2}{24}\left[5+3\frac{(q^K_\nu)^2}{q^2_\parallel}\right]\right]^{-1} \tag{38b}$$

with $C^0_{\mathrm{L}\nu}$ according to Eq. (29). The normalization condition (7) yields

$$C^2_{\mathrm{L}\nu}=C'^2_2 , \tag{39}$$

$$C^4_{\mathrm{L}\nu}=\left[\frac{C'^2_4C'^4_{24}}{C'^4_{24}-C'^2_2C'^2_4}\right]^{1/2} , \tag{40}$$

$$C^6_{\mathrm{L}\nu}=\left[\frac{1}{C'^2_6}-\frac{C'^2_2}{C'^4_{26}}-\frac{(C^4_{\mathrm{L}\nu})^2}{C^2_{46}}\right]^{-1/2} . \tag{41}$$

C. Discussion of the electric fields

The material constants[45] for GaAs are taken to be $\epsilon_{\infty 1}=10.9$, $\omega_{\mathrm{L}1}=5.496\times10^{13}$ s^{-1}, and $\omega_{\mathrm{T}1}=5.057\times10^{13}$ s^{-1}. In Figs. 1 and 2 we have plotted the spatial dependence of the components $E^m_{\parallel\mathrm{L}1}(\mathbf{q}_\parallel,z)$ and $E^m_{z\mathrm{L}1}(\mathbf{q}_\parallel,z)$ of the electric field of the LO phonons of a GaAs layer. Figure 1 shows the symmetric modes. It can be seen that for the component $E^m_{\parallel\mathrm{L}1}$ the fields vanish at the heterointerfaces for both the standard model and the modified one. The field component $E^m_{\parallel\mathrm{L}1}$ of the modified model has no gradient at the heterointerfaces but that of the standard model has a finite gradient. For the modified model the additional constant contribution to the component $E^m_{\parallel\mathrm{L}1}$ [Eqs. (18), (20), and (22)] can be seen in Fig. 1. If we compare the number of extrema for the electric-field component $E^m_{\parallel\mathrm{L}1}$ inside the layer $(-a/2<z<a/2)$ of the standard model with those of the modified model for equal m, we see that these modes are true equivalent modes. The same statement is valid for the antisymmetric modes (Fig. 2). More pronounced is the difference between the two models on the component $E^m_{z\mathrm{L}1}$. Here, the fields are zero at the heterointerfaces for the modified model but nonzero for the standard one.

In Fig. 2, the corresponding electric-field components for the antisymmetric modes are depicted. In contrast to the symmetric modes, the component $E^m_{\parallel\mathrm{L}1}$ depends additionally on a linear function of z. Hence, the deviation of $E^m_{\parallel\mathrm{L}1}$ for both models is more pronounced than for the symmetric modes. The differences between the two models for the component $E^m_{z\mathrm{L}1}$ consist of a zero value at the heterointerfaces for the modified model, in contrast to the standard model, and an additional constant contribution for the modified model.

For both symmetries we see that the additional boundary conditions for $E^m_{z\mathrm{L}1}$ yield a small compression of the electric field perpendicular to the interfaces, so that the wave-vector component q_z of the single LO phonons q^m_1 is a little lowered ($\Delta q_z\leq\pi/a$) if we compare the standard with the modified model. In general, the differences between the fields of the standard and the modified model are lowered with increasing mode number.

In Fig. 3, we give for the modified model a three-dimensional representation of the electric-field component $E^m_{\parallel\mathrm{L}1}(\mathbf{q}_\parallel,z)$ for $m=5$ [compare with Fig. 1(a)] of the symmetric case and for $m=4$ of the antisymmetric case. It can be seen that with increasing $q_\parallel$ the shape of the electric-field component $E^m_{\parallel\mathrm{L}1}$ is changed. This is particularly pronounced for $m=5$, where for increasing $q_\parallel$

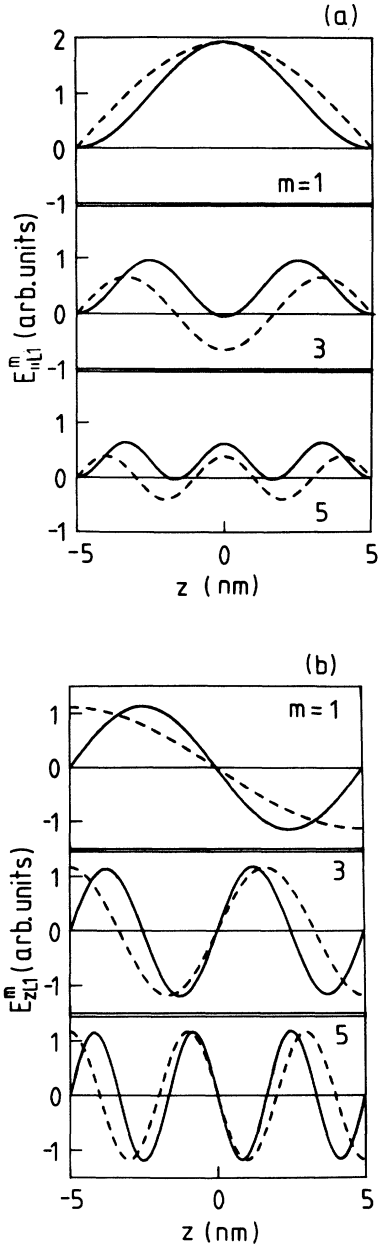

FIG. 1. Spatial dependence of the components of the electric field (a) $E^m_{\|L1}(\mathbf{q}_\|,z)$ and (b) $E^m_{zL1}(\mathbf{q}_\|,z)$ of the symmetric LO phonons of the modified dielectric continuum model (solid lines) and of the standard dielectric continuum model (dashed lines) of a GaAs-AlAs QW with a thickness of the GaAs layer $a=10$ nm for the wave-vector component $q_\|=10^6$ cm^{-1}.

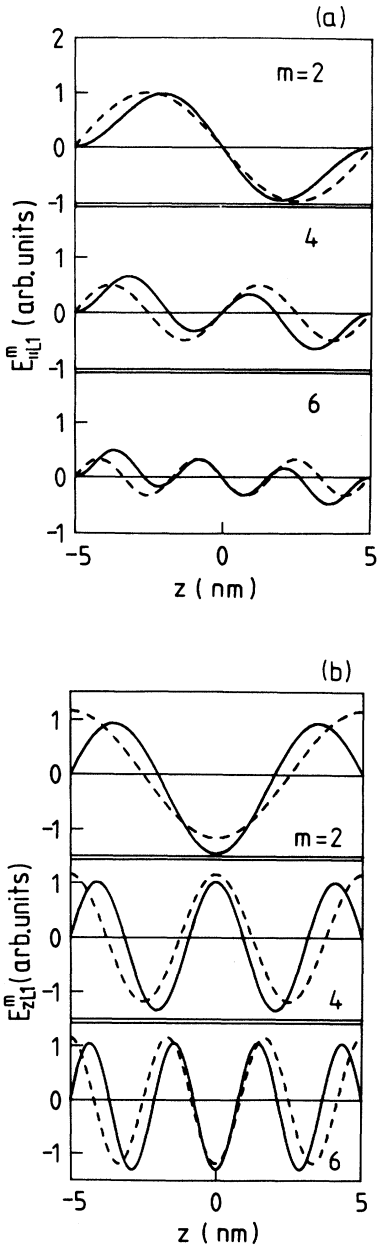

FIG. 2. Spatial dependence of the components of the electric field (a) $E^m_{\|L1}(\mathbf{q}_\|,z)$ and (b) $E^m_{zL1}(\mathbf{q}_\|,z)$ of the antisymmetric LO phonons of the modified dielectric continuum model (solid lines) and of the standard dielectric continuum model (dashed lines) of a GaAs-AlAs QW with a thickness of the GaAs layer $a=10$ nm for the wave-vector component $q_\|=10^6$ cm^{-1}.

the minima drop below zero and the maximum (in the middle of the layer) drops below the outer maxima. These features can be explained by increasing contributions of the lower-index modes [$m=1$ and 3, Eq. (12)] to the orthonormalized mode [$m=5$, Eq. (22)] for increasing $q_\|$.

III. ELECTRON-PHONON INTERACTION AND ELECTRON SCATTERING

The electric fields of the usual confined LO phonons and the modified confined LO phonons satisfy Maxwell's equations of electrostatics and the corresponding bound-

ary conditions. Hence, the Hamiltonian of the EPI in layered systems[21]

$$\hat{H}_{e\text{-ph}}=\sum_j \sum_{\mathbf{q}_\parallel} e^{i\mathbf{q}_\parallel\cdot\mathbf{x}_\parallel}\Gamma_j(\mathbf{q}_\parallel,z)[\hat{a}_j(\mathbf{q}_\parallel)+\hat{a}_j^\dagger(-\mathbf{q}_\parallel)] \quad (42)$$

is valid for both the standard and modified continuum models. In this Hamiltonian, $\Gamma_j(\mathbf{q}_\parallel,z)$ is the coupling function of the jth long-wave optical-phonon mode characterized by the dispersion relation $\omega_j(\mathbf{q}_\parallel)$ and the longitudinal part $E_\parallel^j(\mathbf{q}_\parallel,z)$ of the macroscopic electric field. The coupling function is given by

$$\Gamma_j(\mathbf{q}_\parallel,z)=-\frac{i}{q_\parallel}\left[\frac{\epsilon_0 e^2\hbar}{2A\omega_j(\mathbf{q}_\parallel)}\right]^{1/2} E_\parallel^j(\mathbf{q}_\parallel,z) \quad (43)$$

and describes the coupling strength of a single electron at the position z with the jth long-wave optical-phonon mode, which has the creation (destruction) operator $\hat{a}_j^\dagger$ ($\hat{a}_j$). The sum over j includes both LO and interface phonon modes. Here, we are only interested in the contribution of LO phonons. For the contribution of the interface phonons, the reader is referred to Refs. 21, 22, and 30. The electric-field component $E_\parallel^j$ is given by (5) and (18), (20), (22), and (30), (32), and (34).

In the following we want to calculate the scattering rates of electrons interacting with LO phonons in quantum wells. The scattering rates are normally calculated via Fermi's golden rule with the Hamiltonian (42). For a quasi-free-electron of the Kth electric subband according to the confinement on the electron motion in the z direction, the scattering rate by LO phonons in layer ν is given by

$$W_K(\mathbf{k}_\parallel)=\frac{2\pi}{\hbar}\sum_{\mathbf{q}_\parallel}\sum_{K'}\sum_{\sigma=\pm}\sum_m |M_{K'K}^{\mathrm{L}\nu,m}(\mathbf{q}_\parallel)|^2[n_B(\omega_{\mathrm{L}\nu})+\tfrac{1}{2}+\sigma\tfrac{1}{2}]\delta(E_K(\mathbf{k}_\parallel)-E_{K'}(\mathbf{k}_\parallel-\sigma\mathbf{q}_\parallel)-\sigma\hbar\omega_{\mathrm{L}\nu}) \; . \quad (44)$$

Here, $E_K(\mathbf{k}_\parallel)=\mathcal{E}_K(\mathbf{k}_\parallel)+\hbar^2k_\parallel^2/2m_1$ is the electron energy, which consists of the subband energy $\mathcal{E}_K(\mathbf{k}_\parallel)$ ($K=0,1,2,\ldots$) in the effective-mass approximation and the kinetic energy $E_{\mathrm{kin}}(\mathbf{k}_\parallel)=\hbar^2k_\parallel^2/2m_1$, $n_B(\omega_{\mathrm{L}\nu})$ is the Bose occupancy factor of the LO phonons, and $\sigma=+$ ($-$) corresponds to the emission (absorption) of a LO phonon. The matrix element is

$$M_{K'K}^{\mathrm{L}\nu,m}(\mathbf{q}_\parallel)=\sqrt{A}\int dz\,\varphi_{K'}^*(z)\Gamma_{\mathrm{L}\nu}^m(\mathbf{q}_\parallel,z)\varphi_K(z) \; , \quad (45)$$

where $\varphi_K(z)$ are the envelope wave function for the confined one-electron motion in the z direction. For further calculations we use a square-well confining potential for the electrons formed by a QW. The QW consists of the smaller-gap semiconductor GaAs in $-a/2<z<a/2$, which is symmetrically embedded between the wider-gap semiconductor AlAs in the regions $|z|>a/2$.

A standard quantum-mechanical treatment leads to the following dispersion relation for the bound states of the QW:

$$\frac{m_1\kappa_{2K}}{m_2\kappa_{1K}}=\begin{cases}\tan(\kappa_{1K}a/2) & \text{for symmetric states}\\ -\cot(\kappa_{1K}a/2) & \text{for antisymmetric states}\end{cases} , \quad (46)$$

where m_1 and m_2 are the effective masses of the electrons in the QW region and the barrier regions, respectively. κ_{1K} and κ_{2K} are related to the energy eigenvalue $\mathcal{E}_K(\mathbf{k}_\parallel)$ by

$$\kappa_{1K}=\left[\frac{2m_1}{\hbar^2}\mathcal{E}_K(\mathbf{k}_\parallel)\right]^{1/2} , \quad (47)$$

$$\kappa_{2K}=\left[\frac{2m_2}{\hbar^2}[V_0-\mathcal{E}_K(\mathbf{k}_\parallel)]+\frac{m_1-m_2}{m_1}k_\parallel^2\right]^{1/2} , \quad (48)$$

where V_0 is the energy barrier at the heterointerfaces. The envelope wave functions of the symmetric states

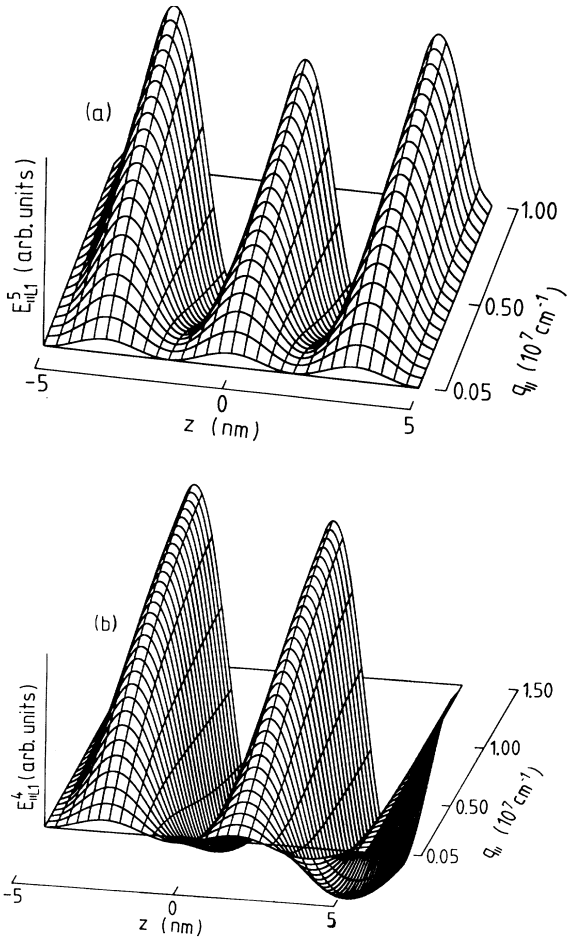

FIG. 3. Three-dimensional representation of the electric-field component $E_{\parallel\mathrm{L}1}^m(\mathbf{q}_\parallel,z)$ of the symmetric $m=5$ LO phonons (a) and the antisymmetric $m=4$ LO phonons (b) of the modified dielectric continuum model of a GaAs-AlAs QW with a thickness of the GaAs layer $a=10$ nm.

($K=0,2,4,\ldots$) are

$$\varphi_K(z)=C_K\times\begin{cases}e^{-\kappa_{2K}(z-a/2)}, & z>a/2\\ \dfrac{\cos(\kappa_{1K}z)}{\cos(\kappa_{1K}a/2)}, & a/2>z>-a/2\\ e^{\kappa_{2K}(z+a/2)}, & -a/2>z\end{cases}\tag{49}$$

and for the antisymmetric states ($K=1,3,5,\ldots$)

$$\varphi_K(z)=C_K\times\begin{cases}e^{-\kappa_{2K}(z-a/2)}, & z>a/2\\ \dfrac{\sin(\kappa_{1K}z)}{\sin(\kappa_{1K}a/2)}, & a/2>z>-a/2\\ -e^{\kappa_{2K}(z+a/2)}, & -a/2>z\end{cases}\tag{50}$$

with the normalization constant

$$C_K=\begin{cases}\left[\dfrac{1}{\kappa_{1K}}+\dfrac{a}{2\cos^2(\kappa_{1K}a/2)}+\dfrac{m_1\kappa_{2K}}{m_2\kappa_{1K}^2}\right]^{-1/2}, & K=0,2,4,\ldots\\ \left[\dfrac{1}{\kappa_{1K}}+\dfrac{a}{2\sin^2(\kappa_{1K}a/2)}+\dfrac{m_1\kappa_{2K}}{m_2\kappa_{1K}^2}\right]^{-1/2}, & K=1,3,5,\ldots .\end{cases}\tag{51}$$

Using (51), (26)–(28), and (39)–(41) in Eq. (45), the matrix element $M_{K'K}^{\mathrm{L}1,m}$ is given by

$$|M_{K'K}^{\mathrm{L}1,m}|^2=\frac{e^2\hbar}{2\epsilon_0 q_\parallel^2}\frac{\omega_{\mathrm{L}1}^2-\omega_{\mathrm{T}1}^2}{\epsilon_{\infty 1}\omega_{\mathrm{L}1}}|C_K|^2|C_{K'}|^2|C_{\mathrm{L}1}^m|^2|I_m|^2\tag{52}$$

with

$$\begin{aligned}|I_1|^2&=(N_{-1}+N_1)^2,\\ |I_3|^2&=(b_{30}N_{-1}+b_{32}N_1-N_3)^2,\\ |I_5|^2&=(b_{50}N_{-1}+b_{52}N_1+b_{54}N_3+N_5)^2,\end{aligned}\tag{53}$$

for even-parity intersubband and intrasubband scattering contributions, and

$$\begin{aligned}|I_2|^2&=(b_{2,-1}N_0+N_2)^2,\\ |I_4|^2&=(b_{4,-1}N_0+b_{4,1}N_2+N_4)^2,\\ |I_6|^2&=(b_{6,-1}N_0+b_{6,1}N_2+b_{6,3}N_4+N_6)^2,\end{aligned}\tag{54}$$

for odd-parity intersubband scattering contributions. In these equations we have defined

$$N_{-1}=\begin{cases}2\dfrac{m_1}{m_2}\dfrac{\kappa_{2K'}-\kappa_{2K}}{\kappa_{1K'}^2-\kappa_{1K}^2}, & K\neq K'\\ \dfrac{a}{2\cos^2(\kappa_{1K}a/2)}+\dfrac{m_1\kappa_{2K}}{m_2\kappa_{1K}^2}, & K=K';\ K=0,2,4,\ldots\\ \dfrac{a}{2\sin^2(\kappa_{1K}a/2)}+\dfrac{m_1\kappa_{2K}}{m_2\kappa_{1K}^2}, & K=K';\ K=1,3,5,\ldots,\end{cases}\tag{55a}$$

$$N_0=a\frac{m_1}{m_2}\frac{\kappa_{2K'}-\kappa_{2K}}{\kappa_{1K'}^2-\kappa_{1K}^2}+2\frac{\kappa_{1K}^2+\kappa_{1K'}^2+2\dfrac{m_1^2}{m_2^2}\kappa_{2K}\kappa_{2K'}}{(\kappa_{1K'}^2-\kappa_{1K}^2)^2},\tag{55b}$$

for $L=1,3,5$,

$$N_L=(-1)^{(L+1)/2}\frac{4\dfrac{m_1}{m_2}\kappa_{2K}}{4\kappa_{1K}^2-(L+1)^2(\pi/a)^2};\ K=K',\tag{55c}$$

for intrasubband scattering, and

$$N_L=2\frac{[(L+1)\pi/a]^2(\kappa_{2K'}+\kappa_{2K})^2-(\kappa_{1K'}^2-\kappa_{1K}^2)(\kappa_{2K'}-\kappa_{2K})(-1)^{(L-1)/2}\dfrac{m_1}{m_2}}{\{[(L+1)\pi/a]^2-\kappa_{1K'}^2-\kappa_{1K}^2\}^2-4\kappa_{1K'}^2\kappa_{1K}^2},\quad K\neq K'\tag{55d}$$

for intersubband scattering between even-parity states. For intersubband scattering between odd-parity states

$(L=2,4,6)$ we have,

$$N_L=-b_1^L\left[2\left[(q_1^L)^2-\kappa_{1K'}^2-\kappa_{1K}^2-2\frac{m_1^2}{m_2^2}\kappa_{2K'}\kappa_{2K}\right]+a\frac{m_1}{m_2}[(q_1^L)^2(\kappa_{2K'}+\kappa_{2K})-(\kappa_{1K'}^2-\kappa_{1K}^2)(\kappa_{2K'}-\kappa_{2K})]\right]$$
$$\times\{[(q_1^L)^2-\kappa_{1K'}^2-\kappa_{1K}^2]^2-4\kappa_{1K'}^2\kappa_{1K}^2\}^{-1},\quad K\neq K'\ . \tag{55e}$$

If we neglect the nonparabolicity for the subband electron energy resulting from the effective-mass discontinuity at the interfaces, i.e., $\mathcal{E}_K(\mathbf{k}_\parallel)\approx\mathcal{E}_K(\mathbf{0})$, we get, for the scattering rate (44),

$$W_K(\mathbf{k}_\parallel)=0 \tag{56a}$$

for $\mathcal{E}_{K'}-\mathcal{E}_K>-\sigma\hbar\omega_{\mathrm{L1}}$; $\forall k_\parallel<k_{\parallel G}$ with $k_{\parallel G}^2=[(\mathcal{E}_{K'}-\mathcal{E}_K)+\sigma\hbar\omega_{\mathrm{L1}}]/(\hbar^2/2m_1)$ and

$$W_K(\mathbf{k}_\parallel)=\frac{2m_1}{\pi\hbar^3}\sum_m\sum_{K'}\sum_{\sigma=\pm}\int_{q_{\parallel a}}^{q_{\parallel e}}dq_\parallel\frac{q_\parallel|M_{K'K}^{\mathrm{L1},m}(q_\parallel)|^2[n_B(\omega_{\mathrm{L1}})+\frac{1}{2}+\sigma\frac{1}{2}]}{\sqrt{(q_{\parallel e}^2-q_\parallel^2)(q_\parallel^2-q_{\parallel a}^2)}} \tag{56b}$$

for $\mathcal{E}_{K'}-\mathcal{E}_K>-\sigma\hbar\omega_{\mathrm{L1}}$; $\forall k_\parallel\geq k_{\parallel G}$ and $\mathcal{E}_{K'}-\mathcal{E}_K\leq-\sigma\hbar\omega_{\mathrm{L1}}$; $\forall k_\parallel$ with

$$q_{\parallel a}=\left|k_\parallel-\left[k_\parallel^2-\frac{(\mathcal{E}_{K'}-\mathcal{E}_K)+\sigma\hbar\omega_{\mathrm{L1}}}{\hbar^2/2m_1}\right]^{1/2}\right| \tag{57a}$$

and

$$q_{\parallel e}=k_\parallel+\left[k_\parallel^2-\frac{(\mathcal{E}_{K'}-\mathcal{E}_K)+\sigma\hbar\omega_{\mathrm{L1}}}{\hbar^2/2m_1}\right]^{1/2}. \tag{57b}$$

For numerical calculations we use the following material constants:[45] $m_1=0.066\,24m_0$, $m_2=0.087m_0$, and $V_0=206$ meV; m_0 is the free-electron mass. Results for the scattering rate for absorption and emission of LO phonons versus the electron kinetic energy are plotted in Figs. 4 and 5. The electron always starts in the lowest subband $K=0$ but all intrasubband and intersubband contributions are summarized in these figures. In Fig. 4(a) we have depicted the scattering rate for absorption of LO phonons. On the left-hand side, the results for the modified dielectric continuum model can be seen, and on the right-hand side those of the standard model can be seen. It is also shown that for the lowest thickness of the quantum well $a=2.5$ nm in the considered range of the electron kinetic energy only intrasubband scattering takes place. This is valid for both models. In the standard model the scattering is dominated by the scattering with LO phonons $m=1$. The higher modes $(m=3,5,\ldots)$ only have a very small contribution to the scattering rate. We note that the symmetry of the QW provides the selection rules[22] that even-parity phonon modes $(m=1,3,5,\ldots)$ induce only scattering of electrons between subbands with equal parity and odd-parity phonon modes $(m=2,4,6,\ldots)$ induce only scattering of electrons between subbands with opposite parity. In the modified model the higher modes have a larger contribution to the scattering rate than in the standard model, but this contribution also decreases rapidly for increasing mode number. This effect is only pronounced for small layer thicknesses. Higher-mode contributions are not shown in the figure. For larger thicknesses of the QW, $a=10$ and 25 nm, intersubband scattering takes place in

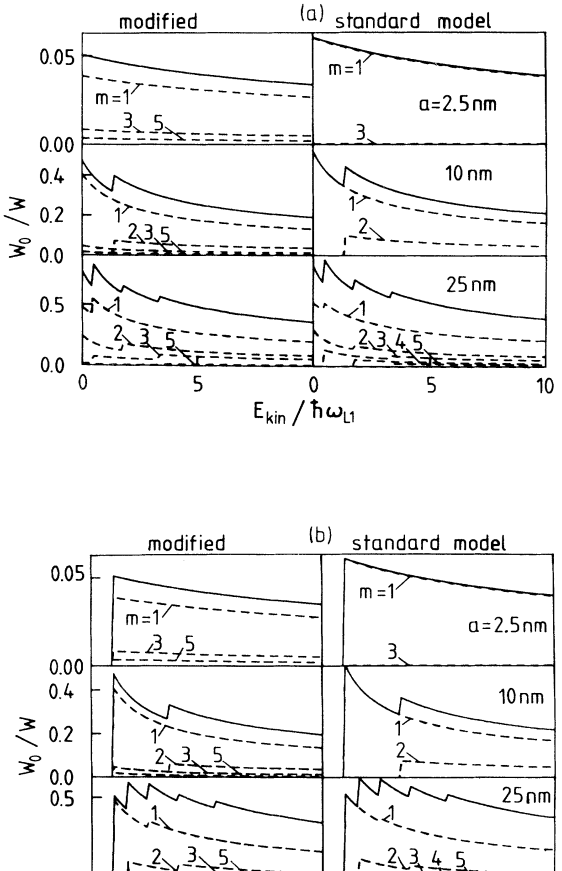

FIG. 4. Scattering rates W_0 (normalized with $W=2\alpha_1\hbar\omega_{\mathrm{L1}}[n_B(\omega_{\mathrm{L1}})+\frac{1}{2}+\sigma\frac{1}{2}]$; ($\alpha_1=0.07$; Fröhlich coupling constant of GaAs)) for the absorption (a) and emission (b) of LO phonons vs electron kinetic energy normalized with $\hbar\omega_{\mathrm{L1}}$ for an electron in the lowest subband of the GaAs-AlAs QW for three different well widths ($a=2.5$, 10, and 25 nm). The solid line is the sum of the scattering rates for the LO phonons with $m=1,\ldots,6$.

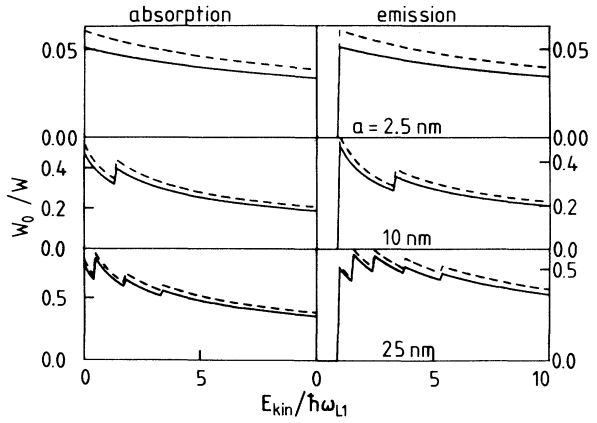

FIG. 5. Scattering rates W_0 of LO phonons of the standard model (dashed lines) and the modified model (solid lines) for an electron in the lowest subband of the GaAs-AlAs QW for three different well widths.

addition to intrasubband scattering.

In Fig. 4(b) we have plotted the scattering rate for the emission of LO phonons. The threshold for the onset of LO phonon emission is at $\hbar\omega_{L1}$ for the scattering with the LO phonons of the GaAs well region. As for absorption, in the case of emission for the smallest thickness of the QW ($a=2.5$ nm) only intrasubband scattering takes place, and for the thicker QW's intersubband scattering takes place as well. In the modified model the contribution of the higher LO phonon modes ($m=2,3,4,\ldots$) is enhanced in comparison with the standard model. In Fig. 5 we compare the scattering rates (summation over all LO phonon contributions $m=1,2,3,\ldots$) for absorption and emission for both models. It can be seen that the scattering rates of the modified model are always a little smaller than those of the standard model, especially for small layer thicknesses.

The modified electrostatic continuum model does not change the scattering rate of an electron with the LO phonons appreciably. The magnitude of the scattering rate is a little lowered. One main difference between the two models is the enhanced influence of the higher-order LO phonons ($m=2,3,4,\ldots$) for the modified model, which can be interpreted as a redistribution of scattering-rate contributions of low-index LO phonon modes to modes with somewhat higher indices.

IV. SUMMARY

In this paper we have developed an improved model of the electron-phonon interaction for LO phonons in semiconductor quantum wells. By using a modified dielectric continuum model with LO phonons having electric and displacement fields that agree with both electrostatics and microscopic models of LO phonons, the scattering rates of electrons for absorption and emission of LO phonons are calculated. It is shown that, for the modified model, the scattering rate is only a little smaller than that for the standard model. In the standard model the scattering rate is dominated by the scattering with the first LO phonon mode. But in the modified model the higher modes have a somewhat larger contribution to the scattering rate than in the standard model. The main effect of the changed LO phonon model concerning the scattering rate of electrons in this considered QW structure is the redistribution of scattering channels from low-index LO phonons to higher-index LO phonons if we compare the standard with the modified LO phonon model. But the sum of all contributions to the scattering rate is almost equal and only a little lowered.

In this paper we have only investigated the modification of LO phonons in thin layers because the interface phonons of the dielectric continuum model agree well with microscopic calculations[34] and experiments. Hence, the total scattering rate is obtained by the sum of the results of this paper with that of Ref. 30, where we also compared our results with the simple LO phonon continuum model.

In Ref. 44 the scattering rate for LO phonons of the modified dielectric continuum model[37] is calculated. But in this paper the different LO phonons have fields that are not orthogonal. This gives incorrect results for the scattering rate. In the paper presented here the LO phonon modes are characterized by orthonormalized fields.

ACKNOWLEDGMENT

The authors wish to express their sincere thanks to Marion Fiedler for numerical and technical assistance.

[1]D. K. Ferry, Surf. Sci. **75**, 86 (1978).
[2]K. Hess, Appl. Phys. Lett. **35**, 484 (1979).
[3]K. Hess and P. Vogl, Solid State Commun. **30**, 807 (1979).
[4]P. J. Price, Ann. Phys. (N.Y.) **133**, 217 (1981); Surf. Sci. **113**, 199 (1982); Phys. Rev. B **30**, 2234 (1984).
[5]B. K. Ridley, J. Phys. C **15**, 5899 (1982).
[6]F. A. Riddoch and B. K. Ridley, J. Phys. C **16**, 6971 (1983).
[7]B. Vinter, Appl. Phys. Lett. **45**, 581 (1984).
[8]B. A. Mason and S. Das Sarma, Phys. Rev. B **35**, 3890 (1987).
[9]M. P. Chamberlein and M. Babiker, Semicond. Sci. Technol. **4**, 691 (1989).
[10]H. Fröhlich, Adv. Phys. **3**, 325 (1954).
[11]M. Born and K. Huang, *Dynamical Theory of Crystal Lattices* (Clarendon, Oxford, 1954).
[12]R. Fuchs and K. L. Kliewer, Phys. Rev. **140**, A2076 (1965).
[13]A. A. Lucas, E. Kartheuser, and R. G. Badro, Phys. Rev. B **2**, 2488 (1970).
[14]V. V. Bryksin and Yu. Firsov, Fiz. Tverd. Tela (Leningrad) **13**, 496 (1971) [Sov. Phys.—Solid State **13**, 398 (1971)].
[15]S. Q. Wang and G. D. Mahan, Phys. Rev. B **6**, 4517 (1972).
[16]E. Evans and D. L. Mills, Phys. Rev. B **8**, 4004 (1973).
[17]J. Licari and R. Evrard, Phys. Rev. B **15**, 2254 (1977).

[18]N. Tzoar, Surf. Sci. **84**, 440 (1979).
[19]E. P. Pokatilov and S. I. Beril, Phys. Status Solidi B **118**, 567 (1983).
[20]R. Lassnig, Phys. Rev. B **30**, 7132 (1984).
[21]L. Wendler, Phys. Status Solidi B **129**, 513 (1985).
[22]L. Wendler and R. Pechstedt, Phys. Status Solidi B **141**, 129 (1987).
[23]L. Wendler and R. Haupt, Phys. Status Solidi B **141**, 493 (1987).
[24]L. Wendler and R. Haupt, Phys. Status Solidi B **143**, 487 (1987).
[25]L. Wendler, R. Haupt, and V. G. Grigoryan, Physica B **167**, 91 (1990).
[26]N. Sawaki, Surf. Sci. **170**, 537 (1986); J. Phys. C **19**, 4965 (1986).
[27]N. Mori and T. Ando, Phys. Rev. B **40**, 6175 (1989).
[28]R. Chen, D. L. Lin, and Th. F. George, Phys. Rev. B **41**, 1435 (1990).
[29]F. A. Riddoch and B. K. Ridley, Physica B+C **134B**, 342 (1985).
[30]L. Wendler, R. Haupt, F. Bechstedt, H. Rücker, and R. Enderlein, Superlatt. Microstruct. **4**, 577 (1988).
[31]M. Babiker, J. Phys. C **19**, 683 (1986); Physica B+C **145B**, 111 (1987).
[32]A. K. Sood, J. Menéndez, M. Cardona, and K. Ploog, Phys. Rev. Lett. **54**, 2111 (1985).
[33]B. Jusserand, D. Paquet, and A. Regreny, Superlatt. Microstruct. **1**, 61 (1985).
[34]E. Richter and D. Strauch, Solid State Commun. **64**, 867 (1987).
[35]S.-F. Ren, H. Chu, and Y.-C. Chang, Phys. Rev. B **37**, 8899 (1988).
[36]H. Chu, S.-F. Ren, and Y.-C. Chang, Phys. Rev. B **37**, 10 746 (1988).
[37]K. Huang and B. Zhu, Phys. Rev. B **38**, 13 377 (1988).
[38]T. Tsuchiya, H. Akera, and T. Ando, Phys. Rev. B **39**, 6025 (1989).
[39]H. Akera and T. Ando, Phys. Rev. B **40**, 2914 (1989).
[40]F. Bechstedt, H. Gerecke, and L. Wendler, *Proceedings of PHONONS '89* (World Scientific, Singapore, 1990), p. 725.
[41]M. V. Klein, IEEE J. Quantum Electron. **QE-22**, 1760 (1986).
[42]B. K. Ridley, Phys. Rev. B **39**, 5282 (1989).
[43]A. K. Sood, J. Menéndez, M. Cardona, and K. Ploog, Phys. Rev. Lett. **54**, 2115 (1985).
[44]S. Rudin and T. L. Reinecke, Phys. Rev. B **41**, 7713 (1990).
[45]S. Adachi, J. Appl. Phys. **58**, R1 (1985).